Synaptic Shot Noise and Conductance Fluctuations Affect the Membrane Voltage with Equal Significance

Magnus J. E. Richardson
magnus.richardson@epfl.ch
Wulfram Gerstner
wulfram.gerstner@epfl.ch
Laboratory of Computational Neuroscience, I&C and Brain-Mind Institute,
Ecole Polytechnique Fédérale de Lausanne, CH-1015 Lausanne EPFL, Switzerland

The subthreshold membrane voltage of a neuron in active cortical tissue is a fluctuating quantity with a distribution that reflects the firing statistics of the presynaptic population. It was recently found that conductance-based synaptic drive can lead to distributions with a significant skew. Here it is demonstrated that the underlying shot noise caused by Poissonian spike arrival also skews the membrane distribution, but in the opposite sense. Using a perturbative method, we analyze the effects of shot noise on the distribution of synaptic conductances and calculate the consequent voltage distribution. To first order in the perturbation theory, the voltage distribution is a gaussian modulated by a prefactor that captures the skew. The gaussian component is identical to distributions derived using current-based models with an effective membrane time constant. The well-known effective-time-constant approximation can therefore be identified as the leading-order solution to the full conductance-based model. The higher-order modulatory prefactor containing the skew comprises terms due to both shot noise and conductance fluctuations. The diffusion approximation misses these shot-noise effects implying that analytical approaches such as the Fokker-Planck equation or simulation with filtered white noise cannot be used to improve on the gaussian approximation. It is further demonstrated that quantities used for fitting theory to experiment, such as the voltage mean and variance, are robust against these non-Gaussian effects. The effective-time-constant approximation is therefore relevant to experiment and provides a simple analytic base on which other pertinent biological details may be added.

1 Introduction

Given a perfect model of the membrane response to synaptic input, it would be possible to infer from the distribution of the subthreshold, membrane-voltage fluctuations many quantities of interest, such as the levels of activity and correlations in the excitatory and inhibitory presynaptic populations.

Early models of synaptic input (Stein, 1965) comprised a leaky integrator driven by a stochastic current, which generated postsynaptic potentials of fixed amplitude. Since then, great effort has been made to incorporate further biological details.

Soon after the publication of Stein's model, synaptic conductance effects began to be addressed (Stein, 1967; Johannesma, 1968; Tuckwell, 1979; Wilbur & Rinzel, 1983; Lansky & Lanska, 1987). These early models featured unfiltered, delta-pulse synapses and were primarily concerned with the statistics of the interspike interval distribution. Although the majority of studies used the diffusion approximation (i.e., the limit of high synaptic rates and low postsynaptic potential amplitudes), the effects of shot noise due to Poisson distributed pulse arrival at low rates have also been considered (see, e.g., Tuckwell, 1989) in the context of stochastic resonance (Hohn & Burkitt, 2001) and the neural response to correlations in the presynaptic population (Kuhn, Aertsen, & Rotter, 2003). Other studies have examined the filtering of the incoming pulses at the synapses and have shown it can lead to unexpected dynamical response properties: synaptic filtering can, paradoxically, allow neurons to follow high-frequency signals better (Brunel, Chance, Fourcaud, & Abbott, 2001; Fourcaud & Brunel, 2002).

More recently, a number of experimental studies have directly measured the effect of synaptic drive on the membrane voltage (Kamondi, Acsady, Wang, & Buzsaki, 1998; Destexhe & Paré, 1999; Sanchez-Vives & McCormick, 2000; Monier, Chavane, Baudot, Graham, & Frégnac, 2003; Holmgren, Harkany, Svennenfors, & Zilberter, 2003). The availability of such measurements has led to a renewed interest in the quantitative modeling of synaptic drive, with a view to infer presynaptic network states from voltage fluctuations (Stroeve & Gielen, 2001; Rudolph, Piwkowska, Badoual, Bal, & Destexhe, 2004), compare current and conductance-based models of synaptic drive (Tiesinga, José, & Sejnowski, 2000; Rauch, La Camera, Lüscher, Senn, & Fusi, 2003; Rudolph & Destexhe, 2003; Jolivet, Lewis, & Gerstner, 2004; Richardson, 2004; La Camera, Senn, & Fusi, 2004; Meffin, Burkitt, & Grayden, 2004), and explore mechanisms for the gain control of the neuronal response (Chance, Abbott, & Reyes, 2002; Burkitt, Meffin, & Grayden, 2003; Destexhe, Rudolph, & Paré, 2003; Fellous, Rudolph, Destexhe, & Sejnowski, 2003; Prescott & De Koninck, 2003; Grande, Kinney, Miracle, & Spain, 2004; Kuhn, Aertsen, & Rotter, 2004).

In this letter, the combined effects on the membrane voltage of synaptic shot noise, filtering, and conductance increase will be examined. The central result is that the effects of synaptic shot noise on the membrane voltage statistics are as significant as those of synaptic conductance fluctuations and therefore either both (or neither) of these features of the synaptic drive should be taken into account for a consistent approach. This means that diffusion-level descriptions, such as numerical simulations or the Fokker-Planck approach, in which the drive is modeled as gaussian noise, cannot correctly describe detailed aspects of the membrane-voltage distribution, such as its skew.

2 Membrane Response to Synaptic Drive

In this section, the full model of the membrane response to synaptic drive is introduced and two common approximations to this model outlined. An analysis of the aspects of the drive missed by these approximation schemes will motivate the development of a perturbative approach.

2.1 The Full Model. Following Stein (1967), the membrane voltage $V(t)$ responds passively to synaptic drive: voltage gated channels, including spike-generating currents, are not included. The membrane is modeled by a capacitance C in parallel with a leak conductance g_L and two fluctuating excitatory $g_e(t)$ and inhibitory $g_i(t)$ conductances with equilibrium potentials at E_L, E_e, and E_i, respectively. This system therefore comprises three independent variables:

$$C\frac{dV}{dt} = -g_L(V - E_L) - g_e(V - E_e) - g_i(V - E_i) + I_{app} \tag{2.1}$$

$$\tau_e\frac{dg_e}{dt} = -g_e + c_e\tau_e\sum_{\{t_{k_e}\}}\delta(t - t_{k_e}) \tag{2.2}$$

$$\tau_i\frac{dg_i}{dt} = -g_i + c_i\tau_i\sum_{\{t_{k_i}\}}\delta(t - t_{k_i}). \tag{2.3}$$

The excitatory conductance is driven by pulses that arrive at the Poisson-distributed times $\{t_{k_e}\}$ at a total rate $\mathcal{R}_e$ summed over all input fibers. Each pulse provokes a quantal conductance increase c_e, which then decays exponentially with a time constant τ_e. The inhibitory conductance is defined analogously. Any experimentally applied current is accounted for by I_{app}.

In this letter, only the steady-state statistical properties will be considered. Thus, all expectations of a quantity $x(t)$, written as $\langle x(t) \rangle$, denote either an average over an ensemble of statistically independent systems, in which any transients due to initial conditions are no longer present, or the temporal average of $x(t)$ in a single system.

2.2 The Diffusion Approximation. For the case in which the rates $\mathcal{R}_e$, $\mathcal{R}_i$ are relatively high, the number of pulses that arrive within the timescales τ_e, τ_i will be approximately gaussian distributed. The replacement of the synaptic shot noise in equations 2.2 and 2.3 by a constant term and gaussian white noise constitutes the diffusion approximation. Thus, using excitation as an example,

$$\tau_e\frac{dg_e}{dt} \simeq g_{e0} - g_e + \sqrt{2}\sigma_e\xi_e(t), \tag{2.4}$$

where the gaussian white noise $\xi_e(t)$ has a mean and autocorrelation function defined by

$$\langle \xi_e(t) \rangle = 0 \qquad \langle \xi_e(t)\xi_e(t') \rangle = \tau_e \delta(t - t'). \tag{2.5}$$

The Ornstein-Uhlenbeck process (see equation 2.4) has been shown to capture the statistics of conductance fluctuations at the soma of compartmentalized model neurons (Destexhe, Rudolph, Fellous, & Sejnowski, 2001). The average conductance g_{e0} and the standard deviation σ_e are related to the variables c_e, τ_e, and $\mathcal{R}_e$ through

$$g_{e0} = c_e \tau_e \mathcal{R}_e, \qquad \sigma_e = c_e \sqrt{\frac{\tau_e \mathcal{R}_e}{2}}. \tag{2.6}$$

By construction, the first two moments of the diffusion approximation are identical to those of the shot noise process. Higher moments, however, are not correctly reproduced in the diffusion approximation.

The conductance equation 2.4 is linear and can be integrated.[1] The fluctuating component g_{eF} of the conductance is

$$g_{eF}(t) \equiv g_e(t) - g_{e0} \simeq \sqrt{2}\sigma_e \int_0^\infty \frac{ds}{\tau_e} e^{-s/\tau_e} \, \xi_e(t - s), \tag{2.7}$$

which yields (with equation 2.5) the gaussian distribution

$$p_D(g_e) = \frac{1}{\sqrt{2\pi\sigma_e^2}} \exp\left(-\frac{(g_e - g_{e0})^2}{2\sigma_e^2}\right). \tag{2.8}$$

The subscript signifies that the calculation was made in the diffusion approximation. There are clearly some problems with distribution 2.8 if the conductance mean g_{e0} is of a similar magnitude to the standard deviation σ_e. In this regime, the diffusion approximation predicts negative conductances (Lansky & Lanska, 1987; Rudolph & Destexhe, 2003). In fact, the criterion for validity of the diffusion approximation is

$$\sigma_e/g_{e0} \ll 1, \tag{2.9}$$

---

[1] The Stratonovich formulation of stochastic calculus is used throughout this letter. However, for additive white noise or multiplicative colored noise, there is no difference between the Stratonovich or Ito forms. See, for example, Risken (1996).

suggesting that this approximation misses higher-order terms scaling with powers of σ_e/g_{e0}. Thus, the shot noise conductance fluctuations should read

$$g_{eF}(t) = \sqrt{2}\sigma_e \int_0^\infty \frac{ds}{\tau_e} e^{-s/\tau_e} \left(\xi_e(t-s) + \text{corrections} \propto \frac{\sigma_e}{g_{e0}} \right), \qquad (2.10)$$

where $\xi_e(t)$ is the gaussian white noise defined in equation 2.5.

2.3 The Diffusion Approximation Is Inconsistent. The combination of the diffusion approximation of the synaptic drive (see equation 2.4 and its equivalent for inhibition) and the full voltage equation, 2.1, will now be examined. By separating the synaptic conductances into tonic components g_{e0}, g_{i0} and fluctuating components g_{eF}, g_{iF}, the voltage equation can be written as

$$C\frac{dV}{dt} = -g_0(V - E_0) - g_{eF}(V - E_e) - g_{iF}(V - E_i), \qquad (2.11)$$

where the total conductance g_0 and drive-dependent equilibrium potential E_0 are defined by

$$g_0 = g_L + g_{e0} + g_{i0} \quad \text{and} \quad E_0 = \frac{1}{g_0}(g_L E_L + g_{e0} E_e + g_{i0} E_i + I_{app}). \qquad (2.12)$$

The subscripts 0 anticipate that these quantities are correct at the zero order of a perturbation expansion that will be developed in a later section. The total conductance g_0 suggests the introduction of an effective membrane time constant,

$$\tau_0 = C/g_0. \qquad (2.13)$$

This feature of the synaptic drive was identified in the early analytic treatment of Johannesma (1968).

The fluctuation terms driving the voltage in equation 2.11 will now be examined. Taking excitation as an example, the voltage-dependent component of the drive can be expanded around the equilibrium potential E_0,

$$g_{eF}(V - E_e) = g_{eF}(E_0 - E_e) + g_{eF}(V - E_0). \qquad (2.14)$$

The two terms on the right-hand side have simple interpretations. The first is an additive noise term and therefore just a fluctuating current. The second is a multiplicative noise term and, in the context of equation 2.11, it can be

seen that this term represents fluctuations in g_0, or equivalently in τ_0, the effective membrane time constant.

These two noise terms are, however, not equally significant. The quantity $V - E_0$ grows (linearly) with the fluctuations g_{eF}, g_{iF}. So whereas the additive noise terms are of the order g_{eF}, g_{iF}, the multiplicative noise terms are of the order g_{eF}^2, g_{iF}^2, and $g_{eF}g_{iF}$. This suggests that (1) the multiplicative noise terms could be neglected if the noise strength was in some way small, and (2) if these terms were retained, the effects of the synaptic drive on the membrane voltage would be modeled in greater detail. Point 1 is valid, as will be seen in section 2.4. Point 2, however, is false due to an unexpected weakness of the diffusion approach with multiplicative noise. This will now be outlined.

On reexamining equations 2.7 to 2.9, it is seen that relative to the tonic conductance, the fluctuations in the diffusion approximation scale with σ_e/g_{e0}. But equation 2.10 states that the terms missed by this approximation scale with the square of this quantity. Hence,

$$g_{eF}/g_{e0} = A\left(\frac{\sigma_e}{g_{e0}}\right) + B\left(\frac{\sigma_e}{g_{e0}}\right)^2 + \cdots \tag{2.15}$$

where A is the diffusion-level term and B is the first-order correction due to shot noise. Given that σ_e/g_{e0} is the small quantity parameterizing the diffusion approximation, it is clearly inconsistent to neglect the second-order term B in the additive noise $g_{eF}(E_e - E_0)$ of equation 2.14 but keep the implicit A^2 term in the multiplicative noise $g_{eF}(V - E_0) \propto g_{eF}^2$. This is, however, what occurs in the diffusion approximation.

This result is surprising because it implies that although diffusion-based approaches (such as the Fokker-Planck equation or any simulation with filtered gaussian noise) purport to capture the effects of synaptic-conductance fluctuations, they miss equally important terms due to the shot noise. However, it should be stressed that almost all previous studies of conductance-based synaptic noise that used the diffusion approximation implicitly concentrated their analyses on the dominant effects coming from the tonic conductance increase and additive noise term; the conclusions of such studies remain valid.

2.4 The Effective-Time Constant Approximation. This is also known as the *gaussian approximation* of the voltage distribution. The treatment of the membrane voltage can easily be made consistent with the diffusion approximation of the synaptic conductance equations. This is achieved by dropping the multiplicative noise term, that is, by neglecting conductance fluctuations, to yield

$$C\frac{dV}{dt} \simeq -g_0(V - E_0) + g_{eF}(E_e - E_0) + g_{iF}(E_i - E_0). \tag{2.16}$$

This voltage equation is of the form of a current-based model, but the dominant effect of the synaptic conductance is accounted for through the use of an increased effective leak g_0. This approximation is in widespread use, having been applied to white noise synaptic drive (Wan & Tuckwell, 1979; Lansky & Lanska, 1987; Burkitt & Clark, 1999; Burkitt, 2001; Burkitt et al., 2003, La Camera et al., 2004), alpha-pulse synapses (Manwani & Koch, 1999), and, more recently (Richardson, 2004), to the case of exponentially filtered synapses studied here. The equation set comprising the voltage equation 2.16 and the diffusion approximations for the conductances are simple to analyze and can be integrated to give

$$V(t) - E_0 \simeq \sqrt{2} \left(\frac{\sigma_e}{g_0} \right) \frac{(E_e - E_0)}{(\tau_e - \tau_0)} \int_0^\infty ds \left(e^{-s/\tau_e} - e^{-s/\tau_0} \right) \xi_e(t - s)$$
$$+ \sqrt{2} \left(\frac{\sigma_i}{g_0} \right) \frac{(E_i - E_0)}{(\tau_i - \tau_0)} \int_0^\infty ds \left(e^{-s/\tau_i} - e^{-s/\tau_0} \right) \xi_i(t - s).$$

(2.17)

This equation has an obvious interpretation: the quantities multiplying the noise are just the excitatory and inhibitory postsynaptic potentials for a membrane with an effective time constant τ_0. The fact that it is linear in the noise means that many quantities of interest can be easily calculated, including temporal measures such as the autocorrelation function.

The distribution predicted for the voltage is the gaussian

$$p_0(V) = \frac{1}{\sqrt{2\pi\sigma_V^2}} \exp \left(-\frac{(V - E_0)^2}{2\sigma_V^2} \right),$$

(2.18)

where, for the case where there are no correlations between excitation and inhibition, the variance is (Richardson, 2004)

$$\sigma_V^2 = \left(\frac{\sigma_e}{g_0} \right)^2 (E_e - E_0)^2 \frac{\tau_e}{(\tau_e + \tau_0)} + \left(\frac{\sigma_i}{g_0} \right)^2 (E_i - E_0)^2 \frac{\tau_i}{(\tau_i + \tau_0)}.$$

(2.19)

If the limit $\tau_e, \tau_i \to 0$ is correctly taken (by keeping the quantities $c_e \tau_e / C$ and $c_i \tau_i / C$ fixed), it can be shown that this variance is compatible with previous results derived for the gaussian approximation of white noise conductance-based synaptic drive (Burkitt et al., 2003). However, for filtered noise, the variance in equation 2.19 differs significantly from that derived in Rudolph and Destexhe (2003). In that study, a one-dimensional Fokker-Planck equation was used that could not capture the effects of synaptic filtering. Through the introduction of effective synaptic time constants (Rudolph et al., 2004), the one-dimensional Fokker-Planck equation can be

made to yield results that correspond, at the gaussian level and in the steady state, to the distribution parameterized by equations 2.12 and 2.19.

2.5 The Aim of This Letter. The gaussian approximation provides a mathematically convenient approach to the analysis of conductance-based synaptic drive and is accurate for parameter values relevant to experiment (Richardson, 2004). Given the analysis presented above, it is clear that to improve on the gaussian approximation, both shot noise and conductance fluctuations must be included. The goal of the next two sections will be to develop a perturbative method that allows for the consistent calculation of the conductance and voltage distributions at a higher order than the gaussian approximation. These higher-order calculations will yield the skew of the voltage distribution, a quantity that is measurable experimentally. More important, the approach will provide information on the validity of fitting gaussian-level analytical forms for the mean and variance to voltage traces of cortical neurons. To aid readability, only the results of the calculations are given in the main body of the article. However, the methods developed here are applicable to other areas of theoretical neuroscience, such as the distribution of amplitudes at depressing synapses (Hahnloser, 2003) or the shape of synaptic weight distributions (van Rossum, Bi, & Turrigiano, 2000; Rubin, Lee, & Sompolinsky, 2001), and are therefore presented in full in the appendixes.

3 Synaptic Shot Noise and Conductance Distributions

In this section, the effects of shot noise on the synaptic conductance distributions will be analyzed. It should be noted that relaxation processes with shot noise, for which equations 2.2 and 2.3 are examples, have been well studied, and an exact solution (Gilbert & Pollak, 1960) for the distribution, in the form of a recursion relation, does exist. However, the aim of the approach (in section 4) is to incorporate the shot-noise conductance fluctuations into a model of the membrane voltage. A perturbative approach is better suited to this purpose. For this reason, the full solution for the shot-noise distribution $p_S(g_e)$ will not be presented here but, when needed, will be obtained by numerical simulation of equation 2.2.

3.1 The Diffusion Approximation Misses the Skew. In the limit where the standard deviation σ_e has a similar magnitude to the conductance mean g_{e0}, the diffusion approximation, unlike the full model, predicts negative conductances. A second source of difference between the statistics of shot noise and the diffusion approximation is also seen in the same limit; the distribution of the shot noise conductance becomes skewed, an effect that is obviously missed by the gaussian distribution given in equation 2.8. In order to get some intuition about the skew of the distribution, a
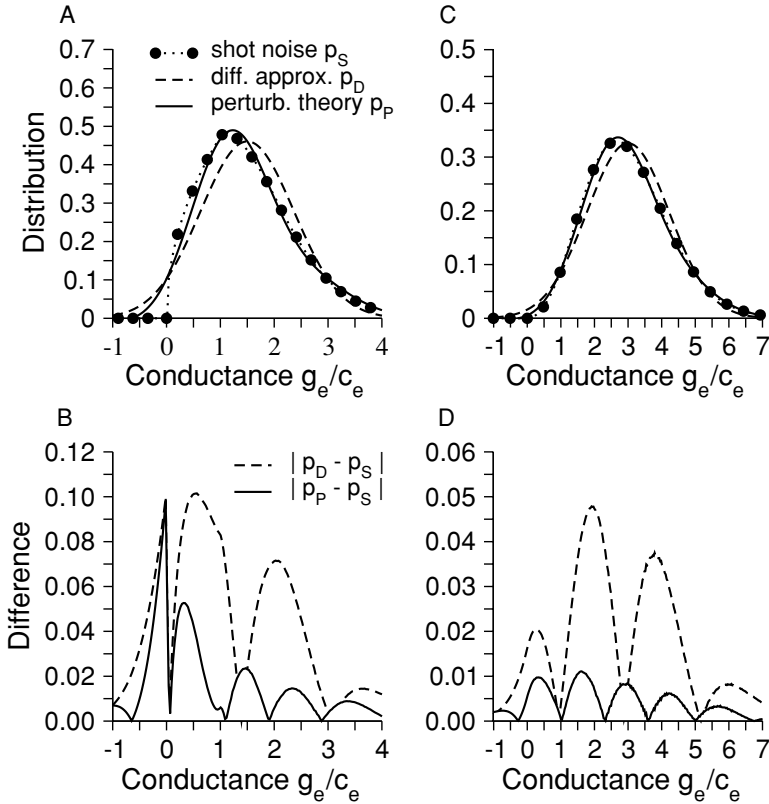
Figure 1: Distribution of shot noise conductance fluctuations; the perturbation theory improves on the diffusion approximation. (A) Comparison of the full distribution p_S generated by the simulation of equation 2.2 to the diffusion approximation p_D (see equation 2.8) and the perturbation theory p_P (see equation 3.4) for the case $\sigma_e/g_{e0} = 0.60$ ($\mathcal{R}_e \tau_e = 1.5$). (B) The corresponding absolute difference between the diffusion approximation and full solution $|p_D - p_S|$ and also the perturbatively generated distribution and the full solution $|p_P - p_S|$. The perturbative distribution reduces the error caused by both the negative conductances and the skew. (C, D) Analogous measures for the case $\sigma_e/g_{e0} = 0.41$ ($\mathcal{R}_e \tau_e = 3.0$) for which the theoretical approaches can be expected to be more accurate. Details of the simulations are given in appendix A.

comparison can be made between the full and approximate distributions shown in Figure 1A. In this case (for which $\mathcal{R}_e \tau_e = 1.5$ implying $\sigma_e/g_{e0} = 0.60$), the peak of the shot noise distribution is to the left of that of the gaussian. Because both distributions have the same mean conductance $g_e/c_e = 1.5$, the shot noise distribution is skewed; it leans to the left with

a longer tail to the right. Any improvement of the diffusion approximation should address both the negative conductivity and the skew of the conductance distribution.

3.2 Accounting for the Shot Noise. The corrections identified in equation 2.10 will now be accounted for. A stochastic variable $\zeta_e(t)$, analogous to gaussian white noise $\xi_e(t)$,

$$\tau_e \frac{dg_e}{dt} \simeq g_{e0} - g_e + \sqrt{2}\,\sigma_e\,\zeta_e(t), \tag{3.1}$$

can be constructed that has statistics that capture the shot noise fluctuations correctly up to the next order missed by the diffusion approximation. It can be shown that such a quantity must obey the same first- and second-order correlators as gaussian white noise,

$$\langle \zeta_e(t) \rangle = 0, \quad \langle \zeta_e(t)\zeta_e(t') \rangle = \tau_e \delta(t - t'), \tag{3.2}$$

but also a new third-order correlator,

$$\langle \zeta_e(t)\zeta_e(t')\zeta_e(t'') \rangle = \sqrt{2}\left(\frac{\sigma_e}{g_{e0}}\right)\tau_e^2\delta(t - t')\delta(t' - t''). \tag{3.3}$$

It is this third-order correlator, proportional to σ_e/g_{e0}, that provides the leading-order correction to the diffusion approximation. All higher-order correlators of products of $\zeta_e(t)$ factorize in terms of these first-, second-, and third-order correlators. Using the rules in equations 3.2 and 3.3, the conductance distribution can be shown (see appendix B) to be

$$p_P(h_e) = \frac{1}{\sqrt{2\pi}}\left[1 + \frac{4}{3}\frac{\sigma_e}{g_{e0}}\left(\frac{h_e^3}{3!} - \frac{h_e}{2!}\right)\right]\exp\left(-\frac{h_e^2}{2}\right), \tag{3.4}$$

where $h_e = (g_e - g_{e0})/\sigma_e$ is the normalized conductance and the subscript P denotes that the result was derived as a perturbative expansion in the small variables σ_e/g_{e0}. The distribution takes the form of a gaussian modulated by a prefactor. To zero order in σ_e/g_{e0}, the prefactor is equal to one, and the gaussian distribution 2.8 is recovered. The prefactor terms proportional to σ_e/g_{e0} now allow for the moments of the distribution to be calculated at higher order. The mean and variance are unchanged, as would be expected given the previous comments about the exactness of these two moments. The first new result of the perturbation theory is the skew $\mathcal{S}_{ge}$ of the distribution:

$$\mathcal{S}_{ge} = \frac{1}{\sigma_e^3}\langle (g_e - g_{e0})^3 \rangle = \langle h_e^3 \rangle = \frac{4}{3}\frac{\sigma_e}{g_{e0}}. \tag{3.5}$$

A useful aspect of the perturbation theory is that this skew is exact. The distribution itself and its higher moments are, however, correct only at the given order of the series expansion in σ_e/g_{e0}. Two examples comparing the numerically generated conductance distribution p_S, diffusion approximation p_D and perturbation theory p_P, are plotted in Figure 1.

4 The Subthreshold Voltage Distribution

The model of synaptic conductance studied in the previous section can now be incorporated into the membrane voltage equation. This will allow the voltage distribution to be calculated at the next order beyond the gaussian approximation. The method involves a perturbative solution to the voltage equation 2.1, the excitatory synaptic conductance equation 3.1, and its inhibitory analog. For the perturbative calculation of the voltage distribution, it is convenient to use the following small parameters,

$$x_e = \sigma_e/g_0 \quad \text{and} \quad x_i = \sigma_i/g_0, \tag{4.1}$$

which are linearly related (in σ_e, σ_i) to the small parameters of the conductance expansion σ_e/g_{e0} and σ_i/g_{i0}. The calculation for the voltage distribution is given in appendix C and, in terms of $v = V - E_0$, can be written in the form

$$p_P(v) = \frac{1}{\sqrt{2\pi\sigma_V^2}} \left[1 + \frac{v}{\sigma_V} \left(\frac{\mu_V}{\sigma_V} - \frac{\mathcal{S}}{2!} \right) + \frac{v^3}{\sigma_V^3} \frac{\mathcal{S}}{3!} \right] \exp\left(-\frac{v^2}{2\sigma_V^2} \right), \tag{4.2}$$

where the subscript P denotes the perturbatively generated result. The voltage appears only through the ratio v/σ_V, and the other terms μ_V/σ_V and $\mathcal{S}$ are parameters proportional to x_e, x_i: this distribution generates moments $\langle v^m \rangle/\sigma_V^m$ that are correct up to order x_e, x_i.

The quantity μ_V is the leading-order correction to the voltage mean E_0 and stems from the conductance fluctuations only: the shot noise does not influence the mean voltage. The standard deviation, given by equation 2.19, is identical to the gaussian value σ_V and is therefore unaffected by shot noise or multiplicative conductance at this order in the perturbation expansion. Thus,

$$\langle V \rangle - E_0 = \mu_V \quad \text{and} \quad \langle (V - \langle V \rangle)^2 \rangle = \sigma_V^2. \tag{4.3}$$

The third-order moment of the distribution 4.2 gives the skew of the voltage distribution,

$$\frac{1}{\sigma_V^3} \langle (V - \langle V \rangle)^3 \rangle = \mathcal{S} = \mathcal{S}_{SN} + \mathcal{S}_{CF}. \tag{4.4}$$

From the expression given in appendix C, equation C.20, it can be seen that two distinct contributions to the skew naturally arise: one from the shot noise $\mathcal{S}_{SN}$ and a second one from the conductances fluctuations $\mathcal{S}_{CF}$. These two contributions to the skew are equally significant because they are both proportional to x_e, x_i. This illustrates one of the central points of this study: the diffusion approximation of a conductance-based model with multiplicative noise is inconsistent because it misses the shot noise contribution $\mathcal{S}_{SN}$. The full set of equations for μ_V, σ_V, and $\mathcal{S}$ is given in appendix D.

4.1 An Example with Relevance to Experiment. To illustrate the effects of shot noise and conductance fluctuations, a scenario is considered in which the fluctuations due to the inhibitory component of the drive can be neglected. There are two different situations that allow this action to be taken. The first is when inhibition is absent. The second, and more interesting, case is relevant to experiments designed to isolate the effect of excitation on the membrane voltage (Silberberg, Wu, & Markram, 2004). In such experiments, the neuron is hyperpolarized through the injection of current so that the mean voltage E_0 is near the reversal of inhibition E_i. In such cases, the factor $E_i - E_0$ multiplying all inhibitory contributions to membrane fluctuations is relatively small, and such contributions can be dropped without significant loss of accuracy. Inhibition enters only through an increase of the tonic conductance g_0 and the corresponding decrease of the effective time constant τ_0.

For either of these scenarios, the moments that parameterize the distribution in equation 4.2 take the values

$$\mu_V = -x_e^2(E_e - E_0)\frac{\tau_e}{(\tau_e + \tau_0)} \tag{4.5}$$

$$\sigma_V^2 = x_e^2(E_e - E_0)^2\frac{\tau_e}{(\tau_e + \tau_0)} \tag{4.6}$$

$$\mathcal{S}_{SN} = x_e\frac{8}{3}\frac{g_0}{g_{e0}}\frac{(\tau_e + \tau_0)^2}{(\tau_e + 2\tau_0)(2\tau_e + \tau_0)}\sqrt{\frac{\tau_e}{(\tau_e + \tau_0)}} \tag{4.7}$$

$$\mathcal{S}_{CF} = -4x_e\frac{(3\tau_e^2 + 6\tau_e\tau_0 + 2\tau_0^2)}{(\tau_e + 2\tau_0)(2\tau_e + \tau_0)}\sqrt{\frac{\tau_e}{(\tau_e + \tau_0)}}. \tag{4.8}$$

Equations 4.7 and 4.8 give the positive and negative contributions to the skew (see equation 4.4) that come from the shot noise and conductance fluctuations, respectively.

For the case of purely excitatory drive, $g_0 = g_L + g_{e0}$, the relative importance of these contributions can be gauged by examining the ratio

$$\left|\frac{\mathcal{S}_{SN}}{\mathcal{S}_{CF}}\right| = \frac{2}{3}\frac{\tau_L}{(\tau_L - \tau_0)}\left(\frac{(\tau_e + \tau_0)^2}{3(\tau_e + \tau_0)^2 - \tau_0^2}\right), \tag{4.9}$$
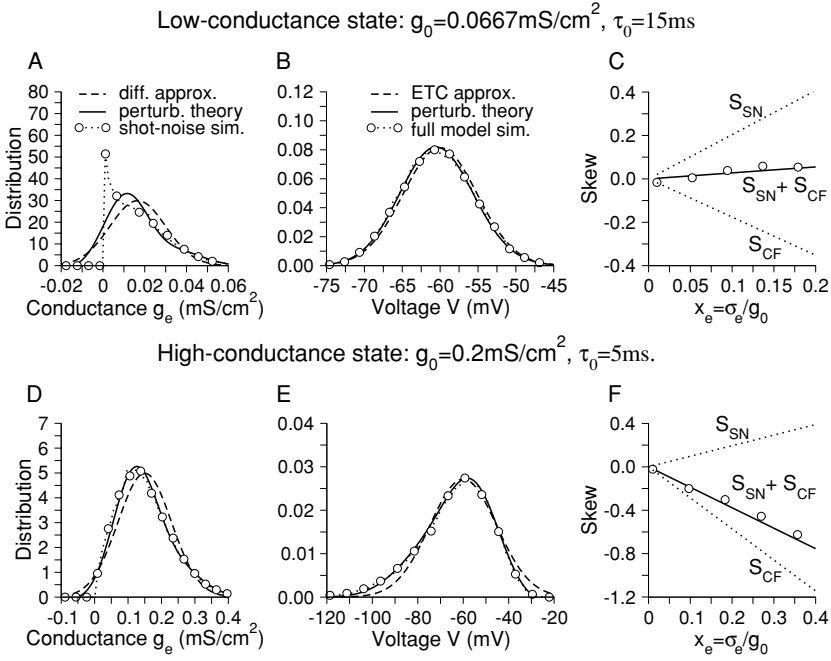
Figure 2: Distribution of the membrane voltage; perturbation theory captures the skew. A neuron is subject to a purely excitatory synaptic drive with a current I_{app} applied such that $E_0 = -60$ mV. (A, B) The conductance and voltage distributions for a low conductance state ($g_{e0} = 0.0167$, $g_L = 0.05$ mS/cm^2) with noise strength $x_e = \sigma_e/g_0 = 0.2$. The perturbative conductance distribution (see equation 3.4) is not accurate because $\sigma_e/g_{e0} = 0.8$. The weak skew of the corresponding voltage distribution (B) is, however, correctly predicted by the perturbation theory (see equation 4.2) because the underlying conductance skew is exact. (C) The voltage skew (see equations 4.7 and 4.8) is plotted as a function of x_e for the same parameters, but with increasing noise σ_e. The shot noise $\mathcal{S}_{SN}$ and conductance-fluctuation $\mathcal{S}_{CF}$ contributions to the skew nearly cancel, explaining the almost gaussian voltage distribution in B. (D, E) A high conductance state ($g_{e0} = 0.15$ mS/cm^2) with $x_e = \sigma_e/g_0 = 0.4$. (E) The large skew of the voltage distribution is captured by the perturbation theory. (F) The voltage skew is negative for the high-conductance case because $\mathcal{S}_{CF}$ dominates. Details of the simulations are given in appendix A.

where $\tau_L = C/g_L$ is the leak time constant. The ratio is a monotonically increasing function of the effective time constant τ_0. In the limit of low conductance states, for which $\tau_0 \to \tau_L$, the ratio diverges, and the contribution due to conductance fluctuations becomes negligible. For high-conductance states, for which $\tau_0 \to 0$, the ratio converges to a constant value of 2/9. These

results underline the fact that the effect of shot noise is nonnegligible: even in extremely high conductance states it still comprises just under a third, $\mathcal{S}_{SN}/\mathcal{S} = 2/7$, of the net skew. These results are illustrated graphically in Figure 2.

5 Discussion

The effect that shot noise synaptic drive has on the membrane voltage distribution was examined. A perturbative approach was developed that was first used to capture the statistics of filtered shot noise conductance fluctuations beyond both the gaussian effective-time-constant approximation and the diffusion approximation. These synaptic conductances were then incorporated into a model of the membrane voltage response. The approach allowed for the analysis of nongaussian features of the voltage distribution, such as its skew. In particular, it was shown that shot noise and synaptic conductance fluctuations affect the membrane at the same order: both effects need to be taken into account for a consistent approach.

The regime in which the effects of shot noise on the voltage and firing rate might be clearly seen experimentally, is one of low presynaptic rate and large, sharp excitatory postsynaptic potentials (EPSPs). This is typical of the excitatory drive experienced by certain neocortical interneurons (Silberberg et al., 2004) for which isolated EPSPs can be many millivolts and there is little dendritic filtering. For a case in which the effects of shot noise are strong (outside the perturbative regime considered here), the voltage distribution can be considerably positively skewed with increased probability to be near threshold. It is expected that in such a case, the statistics of the generated action potentials would differ significantly from those predicted using a gaussian model of the membrane fluctuations with the same mean and variance.

The gaussian, or effective-time constant approximation for the membrane distribution, is, however, mathematically simple: the mean (see equation 2.12) and variance (see equation 2.19) are transparent functions of the model parameters. Such gaussian distributions are therefore ideal to fit to experimental data (Rudolph et al., 2004) in cases where the shot noise effects are weak. The functional form of the distribution that takes into account the shot noise and conductance fluctuations is, however, somewhat less transparent as can be seen in equations D.5 and D.6 for the skew. So the question should be asked: To what extent would weak higher-order effects interfere with an attempt to fit the mean and variance to an experimental distribution? This question can be answered in the framework presented here. First, it is seen from equations 4.5 and D.3 that the correction to the mean voltage due to shot noise and conductance fluctuations is of order x_e^2, x_i^2,

$$\langle V \rangle = E_0 + \mu_V + \cdots = E_0 + O(x_e^2, x_i^2). \tag{5.1}$$

Hence, the mean is not affected at first order. The same is true for the measured variance,

$$\langle (V - \langle V \rangle)^2 \rangle = \langle (V - E_0)^2 \rangle - (\langle V \rangle - E_0)^2 = \sigma_V^2 \big(1 + O(x_e^2, x_i^2)\big), \qquad (5.2)$$

which also increases only with x_e^2, x_i^2, despite the fact that the skew grows linearly with x_e, x_i. These results demonstrate that information extracted from the voltage mean using equation 2.12 and variance using equations 2.19 is not strongly affected by shot noise and conductance fluctuations missed in the gaussian approximation. Hence, fitting the gaussian-level moments to voltage traces is a robust method, given that equations 2.1 and 2.4 and their inhibitory counterpart provide a sufficiently realistic model of the effect of synaptic drive on the membrane voltage.

In summary, the gaussian effective-time-constant approximation provides an accurate description of the voltage fluctuations and is a convenient tool for fitting theory to experiment. For most situations, its description of the stochastic voltage dynamics due to conductance-based synaptic drive is adequate, and it can be easily extended to include many biological details (such as voltage-dependent currents, dynamic synapses, heterogeneity, nontrivial temporal correlations in the drive, and others) missed in the simplified model considered here. Nevertheless, for the purposes of detailed modeling of conductance-based synaptic drive, it should not be overlooked that shot noise and conductance fluctuations are equally important. Our results demonstrate that diffusion-based approaches such as the Fokker-Planck equation or simulation using multiplicative filtered gaussian noise are inadequate for the description of the nongaussian statistics of the voltage. If the aim is to model or simulate the statistics of voltage fluctuations beyond the gaussian, effective-time-constant approximation, then synaptic shot noise must be included.

Appendix A: Details of the Simulations

The parameters used for the simulations were $\tau_e = 3$ ms for the excitatory synaptic filtering, $C = 1 \ \mu\text{F/cm}^2$ for the membrane capacitance, and $g_L = 0.05$ mS/cm^2 for the leak conductance. The reversal potentials used were $E_L = -80$ mV for the leak and $E_e = 0$ mV for synaptic excitation. Simulations were performed using the Euler method with the Poissonian synaptic shot noise implemented by integrating the conductance equation 2.2 to yield

$$g_e(t + dt) = g_e(t) - \frac{dt}{\tau_e} g_e(t) + c_e \mathcal{P}(\mathcal{R}_e dt), \qquad (A.1)$$

where c_e is the postsynaptic conductance amplitude for a single pulse and $\mathcal{R}_e$ is the total rate of incoming pulses. The quantity $\mathcal{P}(\mathcal{R}_e dt)$ is the random

number of incoming pulses that arrive within the time step dt. The number is drawn from a Poisson distribution characterized by the mean $\mathcal{R}_e dt$.

Appendix B: Filtered Poissonian Shot Noise

The method for expanding higher-order gaussian correlators is first reviewed. The first- and second-order correlators are given in equation set 2.5. All higher odd-order correlators vanish, and higher even-order correlators (of order $2n$) factorize into

$$(2n)!/(2^n n!) \tag{B.1}$$

permutations of products of n second-order correlators. As an example, and writing $\xi(t_1) = \xi_1$ for simplicity, the fourth-order correlator is

$$\langle \xi_1 \xi_2 \xi_3 \xi_4 \rangle = \langle \xi_1 \xi_2 \rangle \langle \xi_3 \xi_4 \rangle + \langle \xi_1 \xi_3 \rangle \langle \xi_2 \xi_4 \rangle + \langle \xi_1 \xi_4 \rangle \langle \xi_2 \xi_3 \rangle. \tag{B.2}$$

A fluctuating quantity $\zeta_e(t)$ is now introduced with statistics that are constructed so as to capture the effects of shot noise at a higher order than gaussian white noise $\xi(t)$. The factorization properties of high-order correlators of $\zeta_e(t)$ can be derived from its first-, second-, and third-order correlators defined in equation set 3.2 and equation 3.3. These rules can be derived by expanding the Poissonian distribution of the shot-noise Ornstein-Uhlenbeck equation 2.2 and by keeping terms beyond the usual diffusion approximation (see, e.g., Rodriguez, Pesquera, San Miguel, & Sancho, 1985).

To order σ_e/g_{e0}, higher even-order correlators obey the usual gaussian factorization rules and higher odd-order correlators can be decomposed into permutations of a product of a single third-order correlator and an appropriate number of second-order correlators. As an example, and using the shorthand $\zeta_e(t_1) = \zeta_1$, the seventh-order correlator is factorized as follows:

$$\langle \zeta_1 \zeta_2 \zeta_3 \zeta_4 \zeta_5 \zeta_6 \zeta_7 \rangle = \langle \zeta_1 \zeta_2 \zeta_3 \rangle \langle \zeta_4 \zeta_5 \zeta_6 \zeta_7 \rangle + \text{permutations}, \tag{B.3}$$

where for this case, there are $7 \cdot 6 \cdot 5$ permutations of the indices of the third-order correlator. Each fourth-order correlator can then be decomposed using the usual gaussian rules (see eq. B.2). It is important to note than no further third-order correlators are extracted out of the remaining even-order product. Otherwise, this would produce terms that go beyond the σ_e/g_{e0} correction. Hence, for a $(2n + 3)$-order correlator, there are

$$(2n + 3)(2n + 2)(2n + 1) \cdot \frac{(2n)!}{2^n n!} \tag{B.4}$$

permutations. The first set of three terms comes from the different ways of arranging the single third-order correlator, and the final term comes from the gaussian statistics of the reduction of the remaining even-order correlator.

B.1 The Conductance Distribution and Correlators. The normalized conductance variable $h_e = (g_e - g_{e0})/\sigma_e$ is introduced to simplify the following analysis. It obeys the equation

$$\tau_e \frac{dh_e}{dt} = -h_e + \sqrt{2}\, \zeta_e(t), \tag{B.5}$$

which can be integrated to yield

$$h_e(t) = \sqrt{2} \int_{-\infty}^{t} \frac{ds}{\tau_e} e^{-(t-s)/\tau_e} \zeta_e(s). \tag{B.6}$$

From this, the correlators of the conductance are found to be

$$\langle h_e(t) \rangle = 0$$

$$\langle h_e(t)h_e(t') \rangle = \exp(-|t-t'|/\tau_e)$$

$$\langle h_e(t)h_e(t')h_e(t'') \rangle = \frac{4}{3}\frac{\sigma_e}{g_{e0}} \exp(-|t-t'|/\tau_e)\exp(-|t'-t''|/\tau_e), \tag{B.7}$$

with higher-order correlators derivable from these using the underlying factorization rules for $\zeta_e(t)$.

The steady-state distribution of the variable $h_e(t)$ can be obtained by calculating the probability density that $h_e(t)$ is found having a value near h_e:

$$p(h_e) = \langle \delta(h_e - h_e(t)) \rangle = \int_{-\infty}^{\infty} \frac{dq}{2\pi} e^{-iqh_e} \langle e^{iqh_e(t)} \rangle. \tag{B.8}$$

The exponential is expanded to give

$$\langle e^{iqh_e(t)} \rangle = \sum_{m=0}^{\infty} \frac{(iq)^{2m}}{2m!} \langle h_e^{2m}(t) \rangle + \sum_{m=0}^{\infty} \frac{(iq)^{3+2m}}{(3+2m)!} \langle h_e^{3+2m}(t) \rangle. \tag{B.9}$$

The structure of the correlators allows this to be rewritten as

$$\langle e^{iqh_e(t)} \rangle = \sum_{m=0}^{\infty} \frac{1}{m!} \left(\frac{-q^2}{2}\right)^m \left(1 + (iq)^3 \frac{4\sigma_e}{3g_{e0}}\right)$$

$$= \left(1 + (iq)^3 \frac{4\sigma_e}{3g_{e0}}\right) e^{-q^2/2}, \tag{B.10}$$

which can be inserted into equation B.8,

$$p(h_e) = \left(1 - \frac{4\sigma_e}{3g_{e0}}\frac{d^3}{dh_e^3}\right)\int_{-\infty}^{\infty}\frac{dq}{2\pi}e^{-iqh_e-q^2/2}, \tag{B.11}$$

to yield the distribution given in equation 3.4.

Appendix C: The Membrane Distribution

The statistics of the conductance fluctuations (given in equation 3.1) now are incorporated into a model of a passive membrane (see equation 2.1). For the following analysis, it is convenient to use the shifted voltage $v = (V - E_0)$, with normalized conductances h_e, h_i defined in equations B.5 and B.6,

$$\tau_0 \dot{v} + v(1 + x_e h_e + x_i h_i) = x_e \mathcal{E}_e h_e + x_i \mathcal{E}_i h_i, \tag{C.1}$$

where $\tau_0 = C/g_0$, E_0 are defined by equation 2.12, $\mathcal{E}_e = E_e - E_0$, and $x_e = \sigma_e/g_0$ provides the small parameter used for the perturbative analysis of the voltage (with a similar definition of x_i). Because these small parameters are linearly related to those used for the conductance perturbation theory, corrections due to shot noise and conductance fluctuations will be simultaneously accounted for.

Equation C.1 can be integrated to give

$$v(t) = \int_{-\infty}^{t}\frac{ds}{\tau_0}e^{-(t-s)/\tau_0}\left(\alpha(s)\,e^{-\int_s^t \frac{dr}{\tau_0}\beta(r)}\right), \tag{C.2}$$

where the terms $\alpha(s)$ generate corrections to voltage-like quantities and $\beta(r)$ generates corrections to the effective time constant:

$$\alpha(s) = x_e \mathcal{E}_e h_e(s) + x_i \mathcal{E}_i h_i(s)$$
$$\beta(r) = x_e h_e(r) + x_i h_i(r). \tag{C.3}$$

The voltage distribution can now be obtained by evaluating the expectation

$$p(v) = \langle\delta(v - v(t))\rangle = \int_{-\infty}^{\infty}\frac{dq}{2\pi}e^{-iqv}\langle e^{iqv(t)}\rangle, \tag{C.4}$$

to the appropriate order in x_e and x_i. No correlations are assumed to exist between excitation and inhibition. This simplifying assumption can be relaxed, and the method used here easily extended to account for such correlations.

C.1 The Leading-Order Voltage Distribution. The derivation (Richardson, 2004) of the leading-order contribution to the voltage distribution of equation set 2.1 to 2.3 is first reviewed. The fluctuations of the voltage from its mean value are written as $v(t) = \sigma(t) + O(x_e^2, \; x_i^2)$ where

$$\sigma(t) = \int_{-\infty}^{t} \frac{ds}{\tau_0} e^{-(t-s)/\tau_0} \left(x_e \mathcal{E}_e h_e(s) + x_i \mathcal{E}_i h_i(s) \right). \tag{C.5}$$

In this approximation, the leading-order probability density is a gaussian, as can be seen by examining

$$p_0(v) = \int_{-\infty}^{\infty} \frac{dq}{2\pi} e^{-iqv} \langle e^{iq\sigma(t)} \rangle, \tag{C.6}$$

where the expectation

$$\langle e^{iq\sigma(t)} \rangle = 1 - \frac{q^2}{2} \langle \sigma(t)^2 \rangle + \frac{q^4}{4!} \langle \sigma(t)^4 \rangle \cdots \;\; = \;\; e^{-\frac{1}{2}q^2 \sigma_V^2} \tag{C.7}$$

is evaluated using the gaussian relation $\langle \sigma(t)^{2n} \rangle = (2n)! \langle \sigma(t)^2 \rangle^n / 2^n n!$ At this order, there are no contributions from the shot noise. From equation C.5, the expectation $\langle \sigma^2(t) \rangle = \sigma_V^2$ is time independent and takes the value

$$\sigma_V^2 = x_e^2 \mathcal{E}_e^2 \frac{\tau_e}{(\tau_e + \tau_0)} + x_i^2 \mathcal{E}_i^2 \frac{\tau_i}{(\tau_i + \tau_0)}. \tag{C.8}$$

Reinserting the result, equation C.7, into the probability density,

$$p_0(v) = \exp \left(-\frac{v^2}{2\sigma_V^2} \right) \int_{-\infty}^{\infty} \frac{dq}{2\pi} \exp \left(-\frac{\sigma_V^2}{2} \left(q - i \frac{v}{\sigma_V^2} \right)^2 \right), \tag{C.9}$$

and evaluating the integral gives a gaussian voltage distribution:

$$p_0(V) = \frac{1}{\sqrt{2\pi \sigma_V^2}} \exp \left(-\frac{(V - E_0)^2}{2\sigma_V^2} \right). \tag{C.10}$$

C.2 The Next-Order Correction to the Distribution. From the previous section, it is seen that the typical difference between the voltage and its mean scales with x_e, x_i. To develop a systematic expansion, the dimensionless variable $y = v/\sigma_V$ is therefore introduced. At the next order, the expansion

can be written

$$y(t) = \sigma_y(t) - \phi_y^2(t) + O(x_e^2, \; x_i^2) + \cdots,$$

where $\sigma_y(t) = \sigma(t)/\sigma_V$ and ϕ_y^2 takes the form

$$\phi_y^2(t) = \frac{1}{\sigma_V} \int_{-\infty}^{t} \frac{ds}{\tau_0} e^{-\frac{(t-s)}{\tau_0}} \int_{s}^{t} \frac{dr}{\tau_0} \alpha(s)\beta(r). \tag{C.11}$$

This gives the probability density correct to order $x_e, \; x_i$ as

$$p_0(y) + p_1(y) = \int_{-\infty}^{\infty} \frac{dq}{2\pi} e^{-iqy} \langle e^{iq(\sigma_y(t) - \phi_y^2(t))} \rangle.$$

Again the exponential within the expectation will be expanded and then evaluated to first order in ϕ_y^2:

$$\langle e^{iq(\sigma_y(t) - \phi_y^2(t))} \rangle = \sum_{m=0}^{\infty} \frac{(iq)^{2m}}{(2m)!} \langle \sigma_y^{2m} \rangle + \sum_{m=0}^{\infty} \frac{(iq)^{3+2m}}{(3+2m)!} \langle \sigma_y^{3+2m} \rangle$$

$$- \sum_{m=0}^{\infty} \frac{(iq)^{1+2m}}{(2m)!} \langle \sigma_y^{2m} \phi_y^2 \rangle + O(x_e^2, \; x_i^2). \tag{C.12}$$

The first term on the right-hand side of equation C.12 is the zero-order gaussian component treated above, the second term is the correction due to the Poissonian nature of the noise, and the third term is the correction due to the conductance-based drive.

The second term is straightforward to analyze. Using the rules for the permutation of correlators, this term can be expanded out to give

$$\sum_{m=0}^{\infty} \frac{(iq)^{3+2m}}{(3+2m)!} \langle \sigma_y^{3+2m} \rangle = (iq)^3 \langle \sigma_y^3 \rangle \sum_{m=0}^{\infty} \frac{1}{m!} \left(\frac{-q^2}{2} \right)^m, \tag{C.13}$$

which takes the form of a gaussian with a prefactor.

To obtain the third term of equation C.12, expectations of the form $\langle \sigma_y^{2m} \phi_y^2 \rangle$ need to be calculated. An examination of the structure of the integrals comprising this term shows that they can be written as

$$\langle \sigma_y^{2m} \phi_y^2 \rangle = \langle \sigma_y^{2m} \rangle \langle \phi_y^2 \rangle + 2m \cdot (2m - 1) \langle \psi_y^4 \rangle \langle \sigma_y^{2m-2} \rangle. \tag{C.14}$$

The expectation $\langle \phi_y^2 \rangle$ can be calculated from the form given above, and $\langle \psi_y^4 \rangle$ is defined by

$$\langle \psi_y^4 \rangle = \frac{1}{\sigma^3} \iiint_{-\infty}^{t} \frac{ds_1}{\tau_0} \frac{ds_2}{\tau_0} \frac{ds_3}{\tau_0} \int_{s_3}^{t} \frac{dr_3}{\tau_0} \langle \alpha(s_1) \alpha(s_3) \rangle \langle \alpha(s_2) \beta(r_3) \rangle, \qquad \text{(C.15)}$$

where $\langle \psi_y^4 \rangle \sim O(x_e, x_i)$. An explicit form for this quantity will be given in appendix D. Substitution of the form C.14 into the third term of the expansion C.12 gives

$$\sum_{m=0}^{\infty} \frac{(iq)^{1+2m}}{(2m)!} \langle \sigma_y^{2m} \phi_y^2 \rangle = \left(iq \langle \phi_y^2 \rangle + (iq)^3 \langle \psi_y^4 \rangle \right) \sum_{m=0}^{\infty} \frac{1}{m!} \left(\frac{-q^2}{2} \right)^m. \qquad \text{(C.16)}$$

Inserting the results of equations C.13 and C.16 into the expansion C.12 gives

$$\left\langle e^{iq(\sigma_y(t) - \phi_y^2(t))} \right\rangle = \left(1 + (iq)^3 \langle \sigma_y^3 \rangle - iq \langle \phi_y^2 \rangle - (iq)^3 \langle \psi_y^4 \rangle \right) e^{-\frac{1}{2}q^2}, \qquad \text{(C.17)}$$

where the fact that $\langle \sigma_y^2 \rangle = 1$ has been used. Inserting this into the leading order correction to the distribution,

$$
\begin{aligned}
p_1(y) &= \int_{-\infty}^{\infty} \frac{dq}{2\pi} e^{-iqy} \left((iq)^3 \langle \sigma_y^3 \rangle - iq \langle \phi_y^2 \rangle - (iq)^3 \langle \psi_y^4 \rangle \right) e^{-\frac{1}{2}q^2} \\
&= \left(\langle \phi_y^2 \rangle \frac{d}{dy} + \left(\langle \psi_y^4 \rangle - \langle \sigma_y^3 \rangle \right) \frac{d^3}{dy^3} \right) \int_{-\infty}^{\infty} \frac{dq}{2\pi} e^{-iqy} e^{-\frac{1}{2}q^2} \\
&= -\left(\langle \phi_y^2 \rangle y + \left(\langle \psi_y^4 \rangle - \langle \sigma_y^3 \rangle \right) (y^3 - 3y) \right) \frac{1}{\sqrt{2\pi}} e^{-y^2/2}, \qquad \text{(C.18)}
\end{aligned}
$$

yields the perturbatively generated distribution, correct to order x_e, x_i, with the following functional form,

$$p(y) = \frac{1}{\sqrt{2\pi}} \left(1 + y \left(\mu_y - \frac{S}{2!} \right) + y^3 \frac{S}{3!} \right) \exp \left(-\frac{y^2}{2} \right), \qquad \text{(C.19)}$$

where μ_y is the correction to the mean voltage and S is the skew,

$$\mu_y = \langle y \rangle = -\langle \phi_y^2 \rangle \quad \text{and} \quad S = \langle (y - \langle y \rangle)^3 \rangle = 6 \left(\langle \sigma_y^3 \rangle - \langle \psi_y^4 \rangle \right), \qquad \text{(C.20)}$$

and the equalities hold to first order in the perturbation theory. The first correction to the mean of y is affected only by the synaptic conductance. However, there are two components of the skew $S = S_{SN} + S_{CF}$: a contribution

$\mathcal{S}_{SN} = 6\langle\sigma_y^3\rangle$ from the Poissonian nature of the drive and a contribution $\mathcal{S}_{CF} = -6\langle\psi_y^4\rangle$ from synaptic conductance fluctuations. The functional forms of μ_y and $\mathcal{S}$ will be evaluated by the quantities $\langle\phi_y^2\rangle$, $\langle\sigma_y^3\rangle$ and $\langle\psi_y^4\rangle$ in the next section.

Appendix D: The Voltage Mean and Skew ————————————

At this order in perturbation theory, any of the higher-order cumulants of the voltage distribution can be expressed in terms of the mean μ_y and the skew $\mathcal{S}$,

$$\langle y^{2m}\rangle = \frac{(2m)!}{2^m m!} \quad \text{and} \quad \langle y^{2m+1}\rangle = \frac{(2m+2)!}{2^{m+1}(m+1)!}\left(\mu_y + \frac{m}{3}\mathcal{S}\right), \tag{D.1}$$

where $m = 0, 1, 2\cdots$ Only the odd correlators are different from the gaussian approximation at this order.

D.1 Voltage Mean. The first quantity to be evaluated is the correction to the mean. Because of equation C.20, the integral

$$\langle\phi_y^2\rangle = \frac{1}{\sigma}\int_{-\infty}^{t}\frac{ds}{\tau_0}e^{-\frac{(t-s)}{\tau_0}}\int_{s}^{t}\frac{dr}{\tau_0}\langle\alpha(s)\beta(r)\rangle \tag{D.2}$$

must be evaluated. These integrals can be performed using the equation set B.7 and yield for $\mu_V = \langle v\rangle$:

$$\mu_V = -\left(x_e^2\mathcal{E}_e\frac{\tau_e}{(\tau_e + \tau_0)} + x_i^2\mathcal{E}_i\frac{\tau_i}{(\tau_i + \tau_0)}\right). \tag{D.3}$$

D.2 Voltage Skew: The Poissonian Contribution. Due to equation C.20, this requires the evaluation of

$$\langle\sigma_y^3\rangle = \left(\frac{1}{\sigma}\right)^3\iiint_{-\infty}^{t}\frac{ds\,ds'\,ds''}{\tau_0\,\tau_0\,\tau_0}e^{-\frac{(3t-s-s'-s'')}{\tau_0}}\langle\alpha(s)\alpha(s')\alpha(s'')\rangle, \tag{D.4}$$

which can be performed using the result for the third-order correlator given in equation set B.7. This yields for $\mathcal{S}_{SN} = 6\langle\sigma_y^3\rangle$,

$$\mathcal{S}_{SN} = \frac{1}{\sigma^3}\left(\frac{8\mathcal{E}_e^3\tau_e^3 x_e^4(g_0/g_e)}{3(\tau_e + 2\tau_0)(\tau_0 + 2\tau_e)} + \frac{8\mathcal{E}_i^3\tau_i^3 x_i^4(g_0/g_i)}{3(\tau_i + 2\tau_0)(\tau_0 + 2\tau_i)}\right). \tag{D.5}$$

D.3 Voltage Skew: The Conductance Contribution. This is given by $-6\langle\psi_y^4\rangle$ and therefore requires the evaluation of the integral given in equation C.15. After some algebraic effort, the result can be written in the form

$$
\begin{aligned}
\mathcal{S}_{CF} = &-\frac{4x_e^4\mathcal{E}_e^3}{\sigma^3}\left(\frac{\tau_e}{\tau_e+\tau_0}\right)^2\left(\frac{(3\tau_e^2+6\tau_e\tau_0+2\tau_0^2)}{(\tau_e+2\tau_0)(2\tau_e+\tau_0)}\right) \\
&-\frac{4x_i^4\mathcal{E}_i^3}{\sigma^3}\left(\frac{\tau_i}{\tau_i+\tau_0}\right)^2\left(\frac{(3\tau_i^2+6\tau_i\tau_0+2\tau_0^2)}{(\tau_i+2\tau_0)(2\tau_i+\tau_0)}\right) \\
&-\frac{2x_e^2x_i^2\mathcal{E}_e^3\mathcal{E}_i\tau_e\tau_i}{\sigma^3(\tau_e+\tau_0)(\tau_i+\tau_0)}\left(2+\frac{(2\tau_e\tau_i+\tau_0(\tau_e+\tau_i))(2\tau_e(\tau_i+\tau_0)-\tau_i\tau_0)}{(2\tau_e+\tau_0)(2\tau_i+\tau_0)(\tau_e\tau_i+\tau_e\tau_0+\tau_i\tau_0)}\right) \\
&-\frac{2x_i^2x_e^2\mathcal{E}_i^3\mathcal{E}_e\tau_i\tau_e}{\sigma^3(\tau_i+\tau_0)(\tau_e+\tau_0)}\left(2+\frac{(2\tau_i\tau_e+\tau_0(\tau_i+\tau_e))(2\tau_i(\tau_e+\tau_0)-\tau_e\tau_0)}{(2\tau_i+\tau_0)(2\tau_e+\tau_0)(\tau_i\tau_e+\tau_i\tau_0+\tau_e\tau_0)}\right).
\end{aligned}
$$
(D.6)

If only one synaptic input type is present or if the average voltage is near the reversal of inhibition such that $\mathcal{E}_i = E_i - E_0 \simeq 0$, this result greatly simplifies. This case is given in equation 4.8 and compared to simulations of the full model in Figure 2.

References

Brunel, N., Chance, F. S., Fourcaud, N., & Abbott, L. F. (2001). Effects of synaptic noise and filtering on the frequency response of spiking neurons. *Phys. Rev. Lett.*, *86*, 2186–2189.

Burkitt, A. N. (2001). Balanced neurons: Analysis of leaky integrate-and-fire neurons with reversal potentials *Biol. Cybern.*, *85*, 247–255.

Burkitt, A. N., & Clark, G. M. (1999). New technique for analyzing integrate and fire neurons. *Neurocomputing*, *26–27*, 93–99.

Burkitt A. N., Meffin, H., & Grayden, D. B. (2003). Study of neuronal gain in a conductance-based leaky integrate-and-fire neuron model with balanced excitatory and inhibitory synaptic input. *Biol. Cybern.*, *89*, 119–125.

Chance, F. S., Abbott, L. F., & Reyes, A. D. (2002). Gain modulation from background synaptic input. *Neuron*, *35*, 773–782.

Destexhe, A., & Paré, D. (1999). Impact of network activity on the integrative properties of neocortical pyramidal neurons in vivo. *J. Neurophysiol.*, *81*, 1531–1547.

Destexhe, A., Rudolph, M., Fellous, J.-M., & Sejnowski, T. J. (2001). Fluctuating synaptic conductances recreate in vivo–like activity in neocortical neurons. *Neuroscience*, *107*, 13–24.

Destexhe, A., Rudolph, M., & Paré, D. (2003). The high-conductance state of neocortical neurons in vivo. *Nature Rev. Neurosci.*, *4*, 739–751.

Fellous, J.-M., Rudolph, M., Destexhe, A., & Sejnowski T. J. (2003). Synaptic background noise controls the input/output characteristics of single cells in an in vitro model of in vivo activity. *Neuroscience*, *122*, 811–829.

Fourcaud, N., & Brunel, N. (2002). Dynamics of the firing probability of noisy integrate-and- fire neurons. *Neural Comput.*, *14*, 2057–2110.

Gilbert, E. N., & Pollak, H. O. (1960). Amplitude distributions of shot noise. *Bell. Syst. Tech. J.*, *39*, 333–350.

Grande, L. A., Kinney, G. A., Miracle G. L., & Spain W. J. (2004). Dynamic influences on coincidence detection in neocortical pyramidal neurons. *J. Neurosci.*, *24*, 1839–1851.

Hahnloser, R. H. R. (2003). Stationary transmission distribution of random spike trains by dynamical synapses. *Phys. Rev. E*, *67*, 022901.

Hohn, N., & Burkitt, A. N. (2001). Shot noise in the leaky integrate-and-fire neuron. *Phys. Rev. E*, *63*, 031902.

Holmgren, C., Harkany, T., Svennenfors, B., & Zilberter, Y. (2003). Pyramidal cell communication within local networks in layer 2/3 of rat neocortex. *J. Physiol. London.*, *551*, 139–153.

Johannesma, P. I. M. (1968). Diffusion models for the stochastic activity of neurons. In E. R. Caianello (Ed.), *Neural networks* (pp. 116–144). New York: Springer.

Jolivet, R., Lewis, T. J., & Gerstner, W. (2004). Generalized integrate-and-fire models of neuronal activity approximate spike trains of a detailed model to a high degree of accuracy. *J. Neurophysiol.*, *92*, 959–976.

Kamondi A., Acsady, L., Wang, X.-J., & Buzsaki, G. (1998). Theta oscillations in somata and dendrites of hippocampal pyramidal cells in vivo: Activity-dependent phase-precession of action potentials. *Hippocampus*, *8*, 244–261.

Kuhn, A., Aertsen, A., & Rotter, S. (2003). Higher-order statistics of input ensembles and the response of simple model neurons. *Neural Comp.*, *15*, 67–101.

Kuhn, A., Aertsen, A., & Rotter, S. (2004). Neuronal integration of synaptic input in the fluctuation-driven regime. *J. Neurosci.*, *24*, 2345–2356.

La Camera, G., Senn, W., & Fusi, S. (2004). Comparison between networks of conductance and current-driven neurons: Stationary spike rates and subthreshold depolarization. *Neurocomputing*, *58–60*, 253–258.

Lansky, P., & Lanska, V. (1987). Diffusion approximation of the neuronal model with synaptic reversal potentials. *Biol. Cybern.*, *56*, 19–26.

Manwani, A., & Koch, C. (1999). Detecting and estimating signals in noisy cable structures, I: Neuronal noise sources. *Neural Comp.*, *11*, 1797–1829.

Meffin, H., Burkitt, A. N., & Grayden, D. B. (2004). An analytical model for the "large, fluctuating synaptic conductance state" typical of neocortical neurons in vivo. *J. Comput. Neurosci.*, *16*, 159–175.

Monier, C., Chavane, F., Baudot, P., Graham, L. J., & Frégnac, Y. (2003). Orientation and direction selectivity of synaptic inputs in visual cortical neurons: A diversity of combinations produces spike tuning. *Neuron*, *37*, 663–680.

Prescott, S. A., & De Koninck, Y. (2003). Gain control of firing rate by shunting inhibition: Roles of synaptic noise and dendritic saturation. *P. Natl. Acad. Sci.*, *100*, 2076–2081.

Rauch, A., La Camera, G., Lüscher, H.-R., Senn, W., & Fusi, S. (2003). Neocortical pyramidal cells respond as integrate-and-fire neurons to in vivo–like input currents. *J. Neurophysiol.*, *90*, 1598–1612.

Richardson, M. J. E. (2004). Effects of synaptic conductance on the voltage distribution and firing rate of spiking neurons. *Phys. Rev. E*, *69*, 051918.

Risken, H. (1996). *The Fokker-Planck equation*. New York: Springer-Verlag.

Rodriguez, M. A., Pesquera, L., San Miguel, M., & Sancho, J. M. (1985). Master equation description of external Poisson white noise in finite systems. *J. Stat. Phys.*, *40*, 669–724.

Rubin, J., Lee, D. D., & Sompolinsky, H. (2001). Equilibrium properties of temporally asymmetric Hebbian plasticity. *Phys. Rev. Lett.*, *86*, 364–367.

Rudolph, M., & Destexhe, A. (2003). Characterization of subthreshold voltage fluctuations in neuronal membranes. *Neural Comput.*, *15*, 2577–2618.

Rudolph, M., Piwkowska Z., Badoual, M., Bal, T., & Destexhe, A. (2004). A method to estimate synaptic conductances from membrane potential fluctuations. *J. Neurophysiol.*, *91*, 2884–2896.

Sanchez-Vives, M. V., & McCormick, D. A. (2000). Cellular and network mechanisms of rhythmic recurrent activity in neocortex. *Nat. Neurosci.*, *3*, 1027–1034.

Silberberg, G., Wu, C. Z., & Markram, H. (2004). Synaptic dynamics control the timing of neuronal excitation in the activated neocortical microcircuit. *J. Physiol-London*, *556*, 19–27.

Stein, R. B. (1965). A theoretical analysis of neuronal activity. *Biophys. J.*, *5*, 173–193.

Stein, R. B. (1967). Some models of neuronal variability. *Biophys. J.*, *7*, 37–68.

Stroeve, S., & Gielen, S. (2001). Correlation between uncoupled conductance-based integrate-and-fire neurons due to common and synchronous presynaptic firing. *Neural. Comp.*, *13*, 2005–2029.

Tiesinga, P. H. E., José, J. V., & Sejnowski, T. J. (2000). Comparison of current-driven and conductance-driven neocortical model neurons with Hodgkin-Huxley voltage-gated currents. *Phys. Rev. E*, *62*, 8413–8419.

Tuckwell, H. C. (1979). Synaptic transmission in a model for stochastic neural activity. *J. Theor. Biol.*, *77*, 65–81.

Tuckwell, H. C. (1989). *Stochastic processes in the neurosciences*. Philadelphia: SIAM.

van Rossum, M. C. W., Bi, G. Q., & Turrigiano, G. C. (2000). Stable Hebbian learning from spike timing-dependent plasticity. *J. Neurosci.*, *20*, 8812–8821.

Wan, F. Y. M., & Tuckwell, H. C. (1979). The response of a spatially distributed neuron to white noise current injection. *Biol. Cybern.*, *33*, 39–55.

Wilbur, W. J., & Rinzel, J. (1983). A theoretical basis for large coefficient of variation and bimodality in neuronal interspike distribution. *J. Theor. Biol.*, *105*, 345–368.